

FORECASTERS' FORUM

Hail Swaths Observed from Satellite Data and Their Relation to Radar and Surface-Based Observations: A Case Study from Iowa in 2009

KEVIN GALLO

NOAA/NESDIS/Center for Satellite Applications and Research, Camp Springs, Maryland

TRAVIS SMITH

Cooperative Institute for Mesoscale Meteorological Studies, University of Oklahoma, and NOAA/NSSL, Norman, Oklahoma

KARL JUNGBLUTH

NOAA/NWS/Des Moines Weather Forecast Office, Johnston, Iowa

PHILIP SCHUMACHER

NOAA/NWS/Sioux Falls Weather Forecast Office, Sioux Falls, South Dakota

(Manuscript received 31 August 2011, in final form 13 January 2012)

ABSTRACT

Several storms produced extensive hail damage over Iowa on 9 August 2009. The hail associated with these supercells was observed with radar data, reported by surface observers, and the resulting hail swaths were identified within satellite data. This study includes an initial assessment of cross validation of several radar-derived products and surface observations with satellite data for this storm event. Satellite-derived vegetation index data appear to be a useful product for cross validation of surface-based reports and radar-derived products associated with severe hail damage events. Satellite imagery acquired after the storm event indicated that decreased vegetation index values corresponded to locations of surface reported damage. The areal extent of decreased vegetation index values also corresponded to the spatial extent of the storms as characterized by analysis of radar data. While additional analyses are required and encouraged, these initial results suggest that satellite data of vegetated land surfaces are useful for cross validation of surface and radar-based observations of hail swaths and associated severe weather.

1. Introduction

Satellite observations of the impact of severe storms on land surface features have been previously documented (e.g., Klimowski et al. 1998; Bentley et al. 2002; Yuan et al. 2002; Parker et al. 2005; Segele et al. 2005; Jedlovec et al. 2006). Hail swaths (also referred to as “hail scars” or “hail streaks”) from severe storms have been associated with damage to agricultural crops that has resulted in the monetary loss of crop value. The amount of crop value loss due to hail within the United States in 2009 was over

\$364 million while losses due to damage of homes, vehicles, and other property amounted to over \$1.4 billion [National Oceanic and Atmospheric Administration/Storm Prediction Center (NOAA/SPC); http://www.spc.noaa.gov/wcm/data/2009_hail.csv]. Additionally, the damaged or destroyed vegetation that can result from hail events has been linked to changes in local temperatures within and near the damaged areas (Parker et al. 2005; Segele et al. 2005).

The severe storm events of 9 August 2009 in Iowa were selected for analysis as they resulted in an estimated loss of \$169.6 million in hail damage to agricultural crops, with \$22.1 million in additional property losses attributed to hail damage (NCDC 2011). Reports of hail size observed during the 9 August 2009 storm

Corresponding author address: Kevin Gallo, USGS/EROS Center, 47914 252nd St., Sioux Falls, SD 57198-0001.
E-mail: kevin.p.gallo@noaa.gov

TABLE 1. Storm event information extracted from Storm Event database (NCDC 2011) for 9 Aug 2009. Reported hail and wind measurements have been converted to metric units while the observed damage is documented as in the database. The event sites (A–J) refer to locations within Fig. 1.

Site	Reported hail or wind	Observed damage
A	3.8-cm hail	Hail broke out 2 windows of a house
B	3.2-cm hail	No reports
C	2.5-cm hail, 29 m s ⁻¹ wind	Large trees blown down. A modular home lost part of a roof and west side of the house due to high winds.
D	2.5-cm hail	No reports
E	4.4-cm hail	Spotter reports larger than golf ball size hail. Small branches also blown down by high winds.
F	4.4-cm hail	Windows broken in houses
G	2.5-cm hail	Windshield broken by hail
H	2.5–7.6-cm hail, 40 m s ⁻¹ wind	Four foot diameter tree blow down and some power lines. Large hail broke windows out of a residence and caused considerable crop damage. A communications tower was toppled by the high wind.
I	6.4-cm hail, 34 m s ⁻¹ wind	Grain bins and metal outbuildings were destroyed by high winds
J	2.5-cm hail, 25 m s ⁻¹ wind	Two to three inch diameter branches blow (sic) down. Nickel size hail.

events ranged up to a maximum of 7.6 cm (3.0 in.). Total hail damage to agricultural crops in Iowa during 2009 was in the amount of \$197.4 million, with an additional \$33.5 million in other property damage (NCDC 2011). Thus, the 9 August storms accounted for over 85% of the hail damage to agricultural crops in Iowa during 2009.

The 9 August 2009 hailstorms were part of a very long-lived and isolated thunderstorm system that tracked all the way from Nebraska into Michigan. Across Iowa, there was a singular, very intense thunderstorm updraft that led to the production of very large hail, in combination with damaging winds in excess of 70 miles per hour (mi h⁻¹; where 1 mi h⁻¹ = 0.45 m s⁻¹). The Iowa events occurred between 0700 and 1100 local time (1200 and 1600 UTC), an unusual time of day for intense severe weather. The storms were located 100 km northwest of a stalling cold front that extended from the northeast to southwest across Iowa. The storm location was closely aligned with the 850-hPa cold front and on the north edge of the axis of most unstable convective available potential energy (MUCAPE), with values ranging from 1000 to 2000 J kg⁻¹. This was also within a zone of deep, elevated positive θ_e advection. As storms moved eastward with time and approached the cold front, they were also able to tap stronger, near-surface-based instability. The largest deep shear values were decidedly postfrontal. The bulk vector wind difference from the effective inflow base to one-half of the equilibrium level height exceeded 50 kt (26 m s⁻¹) where the severe weather occurred.

The National Weather Service (NWS) meteorologists utilize both velocity and reflectivity data to assist in the identification of hail within convection. This can include the examination of rotational velocity and the height of critical dBZ values, as described by Blair et al. (2011).

These data are also used to create derived products such as those available from the NOAA/National Severe Storms Laboratory (<http://wdssii.nssl.noaa.gov/>), which provides the predicted location and other ancillary information (e.g., estimates of hail size) associated with hail events. Additional data and products are anticipated with the deployment of dual-polarization radar (Istok et al. 2009) to NWS forecast offices by 2013.

The objective of this study is to present and discuss an initial assessment of cross validation of radar products and surface observations with satellite data. Cross validation of the various reports and products available to forecasters for storm events could provide valuable assessments of both data and techniques that result in (i) greater use of the available data [e.g., Moderate Resolution Imaging Spectroradiometer (MODIS) or similar sensor data] to identify potential hail swaths and document them, (ii) improvement of the current radar and satellite products, and (iii) development of additional new products and techniques that might result in improved accuracy of the prediction of specific event-related damages especially as new sensors are added to Geostationary Operational Environmental Satellites (GOES) and dual-polarization radar becomes available nationally.

2. Observations and analysis

a. Ground-based reports

Reports of severe-storm-related hail damage, hail size, and other pertinent observations for the storms of 9 August 2009 are available from the storm event database (NCDC 2011) and the National Climatic Data Center's *Storm Data* publication (NCDC 2009). These reports usually include locations of storm events, hail size and wind speed, and additional comments related to

the damage or event. Trapp et al. (2006) review limitations of these ground-based reports related to wind damage; however, they recognized that alternative datasets of surface reports [e.g., the experimental effort described by Ortega et al. (2009)] are limited. The ground-based reports included in this study, with examples of the information typically documented, are included in Table 1. Reports within 15 min for the same location were summarized for that location. The locations of the events included in Table 1 are overlaid on a satellite-derived image displayed in Fig. 1.

b. MODIS satellite data

Satellite data used in this study included 250-m-resolution data acquired by the MODIS sensor on the *Terra* platform as described by Jenkerson et al. (2010) and available from the U.S. Geological Survey (USGS; ftp://emodisftp.cr.usgs.gov/eMODIS/CONUS/). The MODIS data were processed as composites of several dates of data to obtain cloud-free observations of the land surface prior to and after the storm events of 9 August 2009. The sensor values were retained in the composite process for two intervals: 1) prior to the event (28 July–3 August 2009) and 2) after the event (11–17 August 2009), based on several criteria that were used to exclude data with diminished quality. The criteria for data exclusion included the presence of clouds, low sensor view angles, and low solar angles (Jenkerson et al. 2010). The composite value of the normalized difference vegetation index (NDVI) was used in this analysis for identification of hail swaths. The NDVI is a measure of the presence of green vegetation and is often used to assess vegetation conditions. NDVI is computed as

$$\text{NDVI} = (\text{near IR} - \text{visible}) / (\text{near IR} + \text{visible}), \quad (1)$$

where visible (620–670 nm) and near-IR (841–876 nm) are reflectance values of the land surface features as observed by the MODIS sensor.

c. Radar data and products

Radar data and products used in this study of the 9 August 2009 storms included several algorithms, products, and field-developed techniques that predict the presence of large or destructive hail from radar data. The Maximum Expected Size of Hail (MESH) algorithm/product available from the Warning Decision Support System—Integrated Information (WDSS-II; Lakshmanan et al. 2007) was compared to both ground-observed hail reports and satellite-derived NDVI data. Additionally, a forecaster-derived technique found to be an indicator of large (>19 mm or >³/₄ in.) hail (Donavon and

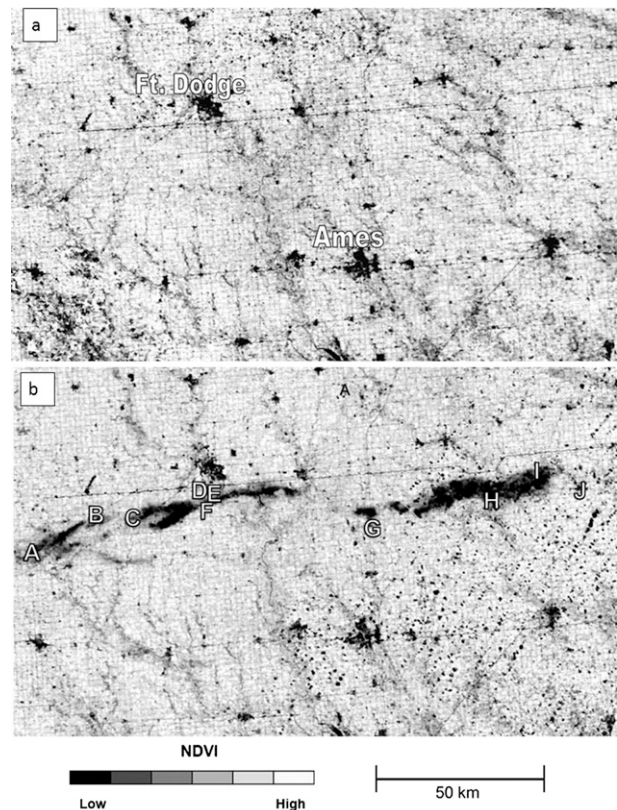


FIG. 1. MODIS composite images for intervals (a) prior to and (b) after the storm event of 9 Aug 2009 with locations of Fort Dodge and Ames identified. Locations of severe storm events identified in Table 1 are identified with station identification (A–J) nominally centered on the locations of reported events.

Jungbluth 2007) was examined. This technique, which identifies locations where the 65-dBZ radar echoes are found at or above 9140 m (30 000 ft) for each Weather Surveillance Radar-1988 Doppler (WSR-88D) volume scan, was also compared with the satellite-derived NDVI data.

Comparisons of storm reports and NDVI included mean NDVI values derived from the before and after storm event images for 3×3 pixel samples of satellite NDVI data centered on the reported storm event locations provided in Table 1. Comparisons of radar data and NDVI data included 1) visual spatial comparisons of the areal extent of the 65-dBZ contour at 9140 m for each volume scan with the approximate hail swath region defined by the MODIS NDVI data and 2) digital comparisons of prior and postevent NDVI value differences with the area extent of estimated hail size at several thresholds as available from the WDSS-II MESH data. The MESH digital dataset (spatial resolution of 0.01° , approximately 1000 m at 40°N latitude) was mapped and resampled with a bilinear algorithm to the

projection and spatial resolution (250 m) of the MODIS data for additional analysis. Surface observed hail reports were also compared with estimates provided by the WDSS-II MESH product.

3. Findings and discussion

a. Surface reports and satellite imagery

The MODIS-derived NDVI image for the interval of 28 July–3 August 2009, prior to the severe storm events of 9 August 2009, is displayed in Fig. 1a. The NDVI image for the interval of 11–17 August 2009 (after the storm events) is displayed in Fig. 1b. Green healthy vegetation cover results in high values of the NDVI (lighter tones) within both figures. The darker (low NDVI) features depicted in Fig. 1a are primarily the nonvegetated surfaces that can include buildings, roads, water bodies, or cloud cover. The cities of Fort Dodge and Ames, Iowa, are identified within Fig. 1a and are visible as darker regions (low NDVI) within both images (dark regions located below city names). The noticeable differences between Figs. 1a and 1b are associated with the hail swaths that resulted from the severe storm events of 9 August 2009. These hail swaths are depicted by the dark (low NDVI) values that span the center of Fig. 1b from left to right across the figure. Locations have been identified in Fig. 1b associated with the reported severe weather events included in Table 1.

The association between the surface reports and satellite imagery was assessed by analysis of the NDVI values at the location of the reported storm events included in Fig. 1b. The NDVI values were evaluated for 3 × 3 image pixels centered on the reported location of the severe storm events (events A–J as listed in Table 1 and identified in Fig. 1b). A general decrease in NDVI values (Table 2) was observed between the before and after event images (as evident in the lower NDVI values displayed in Fig. 1b). Decreased values of NDVI were observed between pre- and poststorm values (Table 2) for all of the surface-reported storm locations. The decrease in NDVI values between the pre- and poststorm images for locations A–J (Fig. 1b) ranged from −0.021 to −0.357 (Table 2). The satellite-derived NDVI appears to provide reasonable validation of the location of the relatively strong surface-reported hail and wind damage events reported in Table 1.

Limitations associated with this analysis include the potential influence of urban areas on the results. The surface features associated with urban areas (e.g., proportionally more concrete and asphalt than vegetation compared to a rural area) typically exhibit low NDVI values (e.g., Fig. 1a). Thus, the decreases in NDVI values within cities or towns due to a hail event would not be

TABLE 2. Storm event locations reported in the Storm Event database (NCDC 2011) and NDVI observed prior to (28 Jul–3 Aug 2009) and after (11–17 Aug 2009) the storm event on 9 Aug 2009 at sites identified in Fig. 1b. Post- minus preevent NDVI values are also provided.

Site	Location	NDVI prior	NDVI post	NDVIpost-prior
A	Yetter	0.897	0.756	−0.141
B	Rockwell City	0.713	0.628	−0.085
C	Sommers	0.824	0.596	−0.228
D	Clay Works	0.712	0.693	−0.019
E	Kalo	0.826	0.724	−0.102
F	Otho	0.776	0.648	−0.128
G	Ellsworth	0.731	0.710	−0.021
H	Eldora	0.769	0.412	−0.357
I	Wellsburg	0.812	0.735	−0.077
J	Grundy	0.582	0.536	−0.046

expected to be as great as the NDVI decreases in rural areas subjected to the same hail event. The post- and prestorm NDVI differences for Eldora, Iowa, provide a good example of this anomaly. The differences between post- and prestorm NDVI values for the 3 × 3 sample centered on the Eldora location ranged from −0.15 to −0.51. The disparity in the NDVI differences was due to the large range in prestorm values (0.54–0.90) compared to poststorm values (0.39–0.50). The individual image pixels of the 3 × 3 sample located within or on the fringe of the city of Eldora exhibited a relatively small decrease in pre- and poststorm NDVI due to the relatively low prestorm NDVI value (e.g., 0.54) compared to the more rural pixels (e.g., 0.90).

Other limitations and concerns associated with this analysis include the potential locational inconsistency and incomplete spatial representation of the surface reports of hail. Trapp et al. (2006) discuss the issue of spatial representation of the storm reports as well as concerns related to locational accuracy. Latitude and longitude determined from a report of an event “3 mi north of town,” for example, would be dependent on the accuracy of the estimated location from town, and if the reference to town was to the “center of town” or the “edge of town” (i.e., spatial extent of the town could be a factor).

b. Radar data and satellite imagery

The approximate areal extent of the satellite-derived hail swaths was defined by an observed decrease in NDVI of greater than −0.15. This value was determined through visual comparisons of several pre- and postevent NDVI difference values for the study area depicted in Fig. 1, with consideration of reported damage (Table 1) and observed NDVI difference values (Table 2). The NDVI-derived areal extent of hail was overlaid on the radar signatures associated with 65-dBZ contours

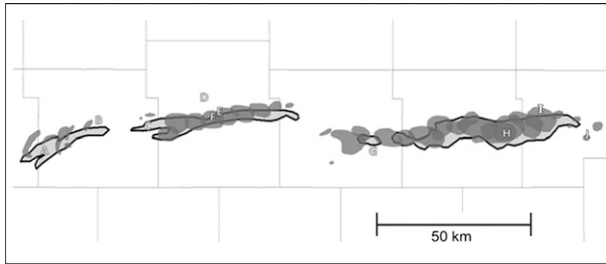


FIG. 2. Areas associated with 65-dBZ contours at 9140 m from WSR-88D volume scans (dark gray) overlaid on the approximate outer boundary of the MODIS-derived hail swath (light gray with black outline). County boundaries are indicated by horizontal and vertical gray lines, and locations of severe storm events identified in Table 1 are indicated.

at 9140 m from WSR-88D volume scans for a visual comparison between the footprints of the satellite and radar data (Fig. 2). The location of the radar footprints appears to lie predominantly within the extent of the satellite-observed decrease in NDVI values that resulted from the storm event. For this case, where Fig. 2 shows that temporal and spatial continuity was preserved, the result suggests that the 65-dBZ contour at 9140 m provided an indication of severe hail that can result in significant damage to crops or other vegetation. For other cases with varied environments, the 9140-m elevation may or may not prove as useful.

An example of how the NDVI products could be used to validate radar techniques and algorithms is demonstrated using the MESH output from 9 August 2009. The extent of MESH-estimated hail size was compared to an image that depicts the differences in NDVI for regions where MESH-estimated hail was greater than zero (Fig. 3). Nearly 77% of the 250-m grid cells that included estimated hail (values greater than 0.0) displayed decreased values in NDVI between the pre- and poststorm event images (Fig. 3). When the estimated hail size criterion was increased to 2.54 cm (1 in.), over 87% of the grid cells exhibited decreased NDVI between the pre- and poststorm images. When the hail size criterion was increased to 5.08 cm (2 in.), over 92% of the grid cells exhibited decreased NDVI after the storm event. Thus, generally good agreement exists between the spatial area of maximum values of the MESH hail product and observed NDVI differences. However, an outline of the region of maximum difference in observed NDVI, overlaid on the MESH hail estimates (Fig. 4), appears to indicate that the maximum NDVI differences exhibited a slight shift to the southeast of the regions of maximum estimated hail size.

While the spatial area of the differences in NDVI appeared to be in good agreement with the spatial extent of the MESH estimates of areas with hail, the results

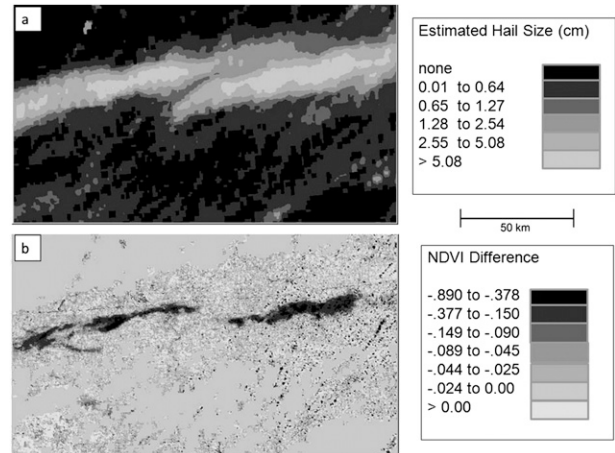


FIG. 3. Hail swaths for region depicted in Fig. 1, derived from (a) estimated hail size from MESH WDSS-II and (b) difference in post- and prestorm NDVI.

of an analysis of the values of estimated hail and differences observed in NDVI for specific locations were not as favorable. A negative correlation ($r = -0.41$) was observed between pre- and poststorm values of NDVI and estimated hail size (MESH hail estimates > 0.0). Thus, greater decreases in pre- and postevent satellite-derived NDVI corresponded to larger MESH estimates of hail size. A significant ($p < 0.001$), but relatively small amount of variation observed in pre- and postevent NDVI was associated with estimated hail size (17%). One explanation for the lack of greater correlation and an explanation of the variation between the estimated hail size and observed differences between pre- and postevent NDVI might come from the observed spatial shift in the region of maximum estimated hail compared to the region of decreases in NDVI greater than -0.15 , as indicated in Fig. 4. This shift (also noted in the radar data presented in Fig. 2) may be attributed to the location of the hail estimates within the atmosphere compared to where the hail ultimately lands on the surface. The MESH hail estimates are based on radar observations of

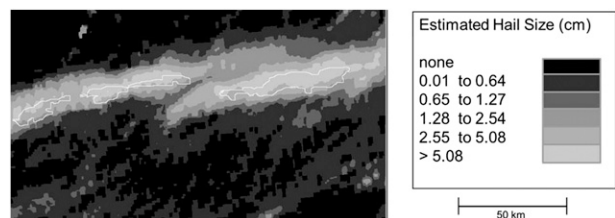


FIG. 4. Outline of maximum difference in observed NDVI after a storm event overlaid on the MESH WDSS-II product. Outlines of NDVI nominally indicate regions with an observed decreases greater than -0.15 between pre- and poststorm NDVI.

hail within the atmosphere and the estimates are mapped vertically (straight) down to the land surface. The location on the land surface where the hail eventually lands may be expected to shift from where mapped from within the middle atmosphere to the land surface.

Wind or wind-driven hail damage may provide an additional explanation of the observed differences between MESH estimates of areas with hail and areas with decreased NDVI. As noted by Changnon (1967), crop damage from hail is usually associated with high winds that also may produce crop damage. Thus, some of the decreased NDVI values may be due to either wind-driven hail or associated with high winds.

c. Surface reports and radar data

The MESH hail estimates of hail size were compared to the ground-observed reports of hail for the 10 locations included in Tables 1 and 2 (and Fig. 1b). Since the MESH product values are the maximum hail estimate for a specific ground location, the MESH data were compared to the maximum reported ground-observed hail reported in Table 1. The MESH values included in the analysis are the average of the 3 × 3 pixel area centered on the reported location of the severe storm event. As displayed in Fig. 5, a wide range of estimated values of hail (2.04–5.44 cm) occurred at the lower range of observed hail (2.54 cm). A general trend of increased MESH hail estimates, however, was observed with increased values of ground-observed hail. Limitations and concerns in this analysis would include the spatial matching issues mentioned in the previous section (i.e., an aloft MESH hail estimate at a particular latitude and longitude cannot be expected to match the surface observation for that particular latitude and longitude). Comparisons of point- and areal-based observations include additional challenges (e.g., often the starting location of a hail event is provided while no ending location is provided).

d. Recommendations for additional analysis

The results of this study suggest several limitations of the current analysis and additional analyses that might improve the use of satellite data for cross validation of surface- and radar-based observations of severe storm events. Limitations and concerns within this analysis include the locational accuracy and spatial representativeness of the surface observations of storm events. As discussed in Trapp et al. (2006), the integration of global positioning system and geographic information system technology into the reporting and documentation of storm events would be helpful in the analysis of these data.

Limitations related to the use of the satellite-derived NDVI data include spurious decreases between pre- and

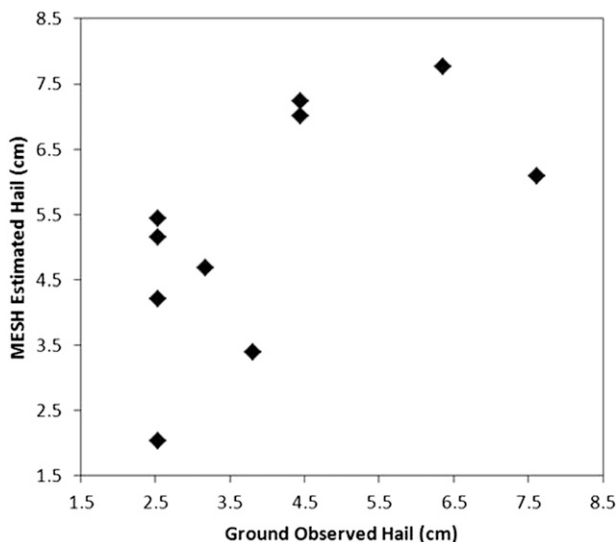


FIG. 5. Estimated hail size from the MESH WDSS-II product compared to ground-observed hail size for the 10 locations included in this study (Table 1).

postevent NDVI values unrelated to storm events (e.g., cloud contamination in the poststorm satellite data). Additionally, the area of decreased NDVI could be due to additional storm event damage beyond hail damage (e.g., wind-driven hail or wind damage). The influence of small towns or nonvegetated surfaces requires consideration in the analysis of decreased pre- and postevent NDVI values. The phenological stage of the agricultural crops will also play a role in the NDVI-observed pre- and poststorm events. The anticipated pre- and poststorm decreases in NDVI would be relatively less, for equivalent storms, for a storm event early in the growing season, when less vegetation is present (e.g., normal vegetation conditions observed in March–April within Iowa), compared to when a full vegetation cover exists during the growing season (e.g., August within Iowa).

The land cover within this study region, as depicted in Fig. 3, was determined from the 2009 MODIS Land Cover Type product (MCD12Q1) available from the National Aeronautics and Space Administration’s (NASA) Land Processes Distributed Active Archive Center (<https://lpdaac.usgs.gov/lpdaac/products>). Cropland or cropland/natural vegetation land cover types accounted for over 99% of the land cover classes within the study region. Thus, in addition to the analysis of more events (a larger sample of surface, radar, and satellite data), future analyses are recommended that include assessments of additional land cover types (forests compared to agricultural crops) and seasonal effects of vegetation (varied stages of vegetation development) on the relationships observed in this study.

The analysis of additional events will likely identify land cover types and times of the year when the satellite data will not be useful due to the lack, or early development stage, of vegetation (e.g., agricultural crops). Associated with the above analysis, a more intensive analysis of the duration of the presence of hail swaths on the land surface might better characterize the boundary layer influence of the hail swaths (e.g., Parker et al. 2005; Segele et al. 2005).

Future analyses could also include additional near-surface radar products that might better match up with the satellite and surface observations compared to the MESH product (derived aloft and mapped vertically to surface). Optimally, future analyses of radar and satellite-derived data would be compared with spatially dense and accurately located surface observations similar to those included in the Severe Hazards Analysis and Verification Experiment (SHAVE), as described by Ortega et al. (2009).

4. Conclusions

Satellite-derived vegetation index (NDVI) data appear to be a useful product for cross validation of surface-based reports, documentation of hail swaths, and radar products associated with severe hail damage events. Decreased NDVI values within the satellite imagery acquired after the storm event corresponded to locations of surface-reported damage. The areal extent of decreased NDVI values also corresponded to the spatial extent of the storms as characterized by radar footprints. While additional analyses are required and suggested, these initial results suggest that satellite data of vegetated land surfaces may provide a useful tool for cross validation of surface and radar-based observations of hail swaths and associated severe weather.

Acknowledgments. The authors thank Jim Vogelmann of the U.S. Geological Survey for calling attention to the hail swaths associated with this storm event, and Kevin Manross, University of Oklahoma–Cooperative Institute for Mesoscale Meteorological Studies, for assistance with acquisition and format details of the MESH data.

This study was partially supported by the NOAA GOES-R program. The manuscript's contents do not constitute a statement of policy, decision, or position on behalf of NOAA or the U. S. government.

REFERENCES

- Bentley, M. L., T. L. Mote, and P. Thebpanya, 2002: Using Landsat to identify thunderstorm damage in agricultural regions. *Bull. Amer. Meteor. Soc.*, **83**, 363–376.
- Blair, S. F., D. R. Deroche, J. M. Boustead, J. W. Leighton, B. L. Barjenbruch, and W. P. Gargan, 2011: A radar-based assessment of the detectability of giant hail. *Electron. J. Severe Storms Meteor.*, **6**. [Available online at <http://ejssm.org/ojs/index.php/ejssm/article/view/87>.]
- Changnon, S. A., Jr., 1967: Areal-temporal variations of hail intensity in Illinois. *J. Appl. Meteor.*, **6**, 536–541.
- Donavon, R. A., and K. A. Jungbluth, 2007: Evaluation of a technique for radar identification of large hail across the Upper Midwest and central plains of the United States. *Wea. Forecasting*, **22**, 244–254.
- Istok, M. J., and Coauthors, 2009: WSR-88D dual polarization initial operational capabilities. Preprints, *25th Conf. on Int. Interactive Information and Processing Systems (IIPS) for Meteorology, Oceanography, and Hydrology*, Phoenix, AZ, Amer. Meteor. Soc., 15.5. [Available online at <http://ams.confex.com/ams/pdfpapers/148927.pdf>.]
- Jedlovec, G. J., U. Nair, and S. L. Haines, 2006: Detection of storm damage tracks with EOS data. *Wea. Forecasting*, **21**, 249–267.
- Jenkerson, C., T. Maiersperger, and G. Schmidt, 2010: eMODIS: A user-friendly data source. USGS Open-file Rep. 2010–2105, 10 pp. [Available online at <http://pubs.usgs.gov/of/2010/1055/pdf/OF2010-1055.pdf>.]
- Klimowski, B. A., M. R. Hjelmfelt, M. J. Bunkers, D. Sedlacek, and L. R. Johnson, 1998: Hailstorm damage observed from the GOES-8 satellite: The 5–6 July 1996 Butte–Meade storm. *Mon. Wea. Rev.*, **126**, 831–834.
- Lakshmanan, V., T. Smith, G. J. Stumpf, and K. Hondl, 2007: The Warning Decision Support System—Integrated Information. *Wea. Forecasting*, **22**, 596–612.
- NCDC, 2009: *Storm Data*. Vol. 51, No. 8, 502 pp.
- , cited 2011: NCDC Storm Event database. [Available online at <http://www4.ncdc.noaa.gov/cgi-win/wwcgi.dll?wwEvent~Storms>.]
- Ortega, K. L., T. M. Smith, K. L. Manross, A. G. Kolodziej, K. A. Scharfenberg, A. Witt, and J. J. Gourley, 2009: The Severe Hazards Analysis and Verification Experiment. *Bull. Amer. Meteor. Soc.*, **90**, 1519–1530.
- Parker, M. D., I. C. Ratcliffe, and G. M. Henebry, 2005: The July 2003 Dakota hailswaths: Creation, characteristics, and possible impacts. *Mon. Wea. Rev.*, **133**, 1241–1260.
- Segele, Z. T., D. J. Stensrud, I. C. Ratcliffe, and G. M. Henebry, 2005: Influence of a hailstreak on boundary layer evolution. *Mon. Wea. Rev.*, **133**, 942–960.
- Trapp, R. J., D. M. Wheatley, N. Atkins, R. W. Przyblinski, and R. Wolf, 2006: Buyer beware: Some words of caution on the use of severe wind reports in postevent assessment and research. *Wea. Forecasting*, **21**, 408–415.
- Yuan, M., M. Dickens-Micozzi, and M. Magsig, 2002: Analysis of tornado damage tracks from the 3 May tornado outbreak using multispectral satellite imagery. *Wea. Forecasting*, **17**, 382–398.